Eur. J. Mech. B - Fluids 19 (2000) 89–107

Coriolis effects on the stability of pulsed flows in a Taylor–Couette geometry

Ahmed Aouidef [a], Christiane Normand [b,*]

[a] *MITI/AIST Mechanical Engineering Laboratory, Biomimetics Division, Tsukuba, Japan*
[b] *C.E.A./Saclay, Service de Physique Théorique, 91191 Gif-sur-Yvette cedex, France*

(Received 8 April 1999; revised 1 September 1999; accepted 2 September 1999)

Abstract – Results steming from the linear stability of time-periodic flows in a Taylor–Couette geometry with cylinders oscillating in phase or out-of-phase are presented. Our analysis takes into account the gap size effects and investigates the influence of a superimposed mean angular rotation of the whole system.

In case of no mean rotation, the finite gap geometry is found to affect the shape of the stability diagrams (critical Taylor number versus the frequency parameter) which consist of two distinct branches as opposed to being continuous in the narrow gap approximation. In particular, in the out-of-phase configuration a new branch for low frequencies was found, thus enabling better agreement with available experimental results.

When cylinders are co-rotating and subject to rotation effects, our calculations provide the evolution of the critical Taylor number versus the rotation number for two values of the frequency. The stability curves are found to be in qualitative agreement with available experimental data revealing a maximum of instability for a rotation number of about 0.3.

In the high rotation regime, enhancement of the critical Taylor number is investigated through an asymptotic analysis and the value of the rotation number at which restabilization occurs is found to depend on the frequency parameter.

A restabilization of the flow also occurs when the rotation number and the gap size are of the same order, a phenomenon already pointed out in the case of steady flows and attributed to the near cancellation of Coriolis and centrifugal effects. Our investigation proves that the same mechanism still holds for time-periodic flows. © 2000 Éditions scientifiques et médicales Elsevier SAS

Taylor–Couette geometry / critical Taylor number / Coriolis force / centrifugal force

1. Introduction

Since they are encountered in a great variety of physical and technological problems, time-periodic flows have received an upsurge interest from researchers concerned with hydrodynamic stability [1]. One can cite many examples of time-periodic flows, for example sinusoidally excited jet stream to form droplets in ink jet printing devices, thermocapillary and buoyant flows under gravitation modulation (g-jitter) in materials processing aboard spacecraft [2], periodic blood flow in the aorta [3]. A first problem of hydrodynamic stability of periodic basic flow was discovered by Faraday [4] in the nineteenth century. He observed a regular pattern of standing waves on the surface of water in a vertically vibrating vessel and noticed that the waves have half the frequency of the vessel. Another representative case of this kind of problem is the stability of a flow induced by the oscillations of a flat plate surmounted by a semi-infinite fluid medium [5] (well known as the Stokes boundary layer problem). Stokes layers might also give rise to other kinds of instabilities of a centrifugal nature in the presence of streamline curvature. In the following, we shall concentrate on the instabilities arising in the flow of a fluid contained between two concentric cylinders assumed to be of infinite length and subject to a time-periodic rotation forcing. The present investigation may be considered as an extension of our previous work on

* Correspondence and reprints; normand@spht.saclay.cea.fr

the subject [6–8] where angular velocities of the inner and outer cylinders were respectively $\Omega_1(t) = \Omega_0 \cos(\omega t)$ and $\Omega_2(t) = \varepsilon\Omega_0 \cos(\omega t)$. Our stability analysis was performed in the small gap approximation for $\varepsilon = \pm 1$ [6,8] and $\varepsilon = 0$ [7]. Comparison with experimental results have shown a satisfactory agreement for $\varepsilon = 1$, whereas some discrepancy in the low-frequency limit was found for $\varepsilon = -1$.

The so-called pulsed flows belong to the larger class of modulated flows where $\Omega_i(t) = \Omega_{mi} + \varepsilon_i \cos(\omega t)$ with $i = 1, 2$. Pioneering investigations were mostly devoted to the case where the outer cylinder is at rest ($\Omega_{m2} = 0$, $\varepsilon_2 = 0$) and later various types of forcing were considered both theoretically and experimentally as for instance in the particular case of steady rotation of the inner cylinder ($\varepsilon_1 = 0$) and sinusoidal oscillation of the outer cylinder around a zero mean ($\Omega_{m2} = 0$) which was recently revisited by Murray et al. [9] in a very comprehensive manner.

The present contribution is devoted to a configuration which has not yet received as much attention, at least from the theoretical point of view, which corresponds to the parameters: $\Omega_{m1} = \Omega_{m2} = \Omega_m$, with $\varepsilon_2 = \pm\varepsilon_1$. Recent experimental results obtained in this configuration [10–12] have been analyzed in the low frequency regime using a quasi-static approach. By applying Floquet theory, our calculations aim at a comparison with experiments on a wider range of values of the frequency. Two equivalent descriptions of the system are allowed whether the frame of reference is choosen to be at rest or rotating at the angular velocity Ω_m. In the laboratory frame, the flow can be assimilated to a modulated flow with the same steady component of the angular velocity on both cylinders. Whereas, in a frame of reference rotating at the angular velocity Ω_m, we shall consider pulsed flows subject to Coriolis acceleration.

For steady flows, the coupling between instabilities induced both by centrifugal and Coriolis forces has been analyzed by Matsson and Alfredssson [13] for a Poiseuille flow in a curved rotating channel. It was shown that terms of the gap size order needed to be kept both in the disturbance equations and in the mean velocity profile. Also, Mutabazi et al. [14] demonstrated later that when restabilization occurs above a certain value of the rotation number, the critical parameters of the system exhibit an asymmetry between the direction of rotation which grows with the gap size. Moreover, finite gap size effects are easy to handle when simple analytical expressions exist for the velocity component of the base flow which can be expanded in ascending powers of the gap size parameter. This is the case for the steady Poiseuille flow in a curved channel and steady circular Couette flow. Though a similar attempt was made for pulsed flows using asymptotic expansion of modified Bessel functions [11,12], this attractive possibility is not of such a decisive interest when the stability analysis has to be made numerically. We shall see later that the confidence in this approximation cannot definitely be assessed on the grounds that it leads to a small error for the velocity profile, without ensuring it is also true for its derivative.

These considerations lead us to perform a numerical derivation of the base flow as explained in Section 2 where the formulation of the stability problem is also reported. Results of the Floquet analysis are presented in Section 3 for $\Omega_m = 0$ and in Section 4 for $\Omega_m \neq 0$. Conclusions are drawn in Section 5.

2. Position of the problem

We consider a Newtonian incompressible fluid of density ρ and kinematic viscosity ν in the annular space between two coaxial cylinders of radii R_1 and $R_2 = R_1 + d$, with d the gap width. The radius ratio $\eta = R_1/R_2$, is used as the characteristic parameter for the geometrical configuration whereas in the narrow gap limit ($\eta \to 1$) the relevant parameter is $\delta \equiv d/R_1 = (1/\eta) - 1$. When referred to a system that rotates with steady angular

velocity $\mathbf{\Omega}$, the flow velocity $\mathbf{v}$ and pressure P fields are described by the following equations [15]:

$$\frac{\partial \mathbf{v}}{\partial t} + (\mathbf{v}.\nabla)\mathbf{v} + 2\mathbf{\Omega} \times \mathbf{v} = -\nabla\left(\frac{P}{\rho}\right) + \nu\Delta\mathbf{v},$$

$$\operatorname{div}\mathbf{v} = 0.$$

Here P is the sum of the usual pressure term and the centrifugal energy $(-\Omega^2 r^2/2)$ associated with the rotation of the frame of reference as a whole. The base flow is induced by the oscillations at the frequency ω of the inner and outer cylinders with respective angular velocity $\Omega_1(t) = \Omega_m + \Omega_0\cos(\omega t)$ and $\Omega_2(t) = \Omega_m + \varepsilon\Omega_0\cos(\omega t)$ (Ω_0, Ω_m are constant angular velocities and $\varepsilon = \pm 1$).

The quantities d and d^2/ν, as scales for length and time respectively, are introduced to get the dimensionless Navier–Stokes equations. Under the assumption of two infinitely long cylinders and owing to rotational symmetry, the base flow in the frame of reference rotating at the angular velocity Ω_m has one component $V_B(r,t)$ in the azimuthal direction, solution of the partial differential equation

$$\frac{\partial V_B}{\partial t} = \frac{\partial^2 V_B}{\partial r^2} + \frac{1}{r}\frac{\partial V_B}{\partial r} - \frac{V_B}{r^2}, \tag{1}$$

where r and t are radial and time variables.

Introducing the frequency parameter $\sigma = \omega d^2/\nu$, and with the base flow expressed in $\Omega_0 R_1$ units, the boundary conditions become:

$$V_B(r_1,t) = \cos(\sigma t), \qquad V_B(r_2,t) = \frac{\varepsilon}{\eta}\cos(\sigma t)$$

at the inner and outer cylinder $r_1 = \eta/(1-\eta)$ and $r_2 = 1/(1-\eta)$, respectively.

The solution is sought as the superposition of two contributions

$$V_B = V_1(r)\cos(\sigma t) + V_2(r)\sin(\sigma t), \tag{2}$$

where $V_1(r)$ and $V_2(r)$ satisfy the system of coupled differential equations

$$-\sigma V_1 = DD_*V_2,$$
$$\sigma V_2 = DD_*V_1,$$

with $D \equiv \partial/\partial r$ and $D_* \equiv \partial/\partial r + 1/r$.

The boundary conditions can now be expressed as

$$V_1(\eta/1-\eta) = 1, \qquad V_2(\eta/1-\eta) = 0,$$
$$V_1(1/1-\eta) = \varepsilon/\eta, \qquad V_2(1/1-\eta) = 0.$$

The determination of the radial functions $V_1(r)$ and $V_2(r)$ of the base flow has been done numerically using a shooting method with a Runge–Kutta scheme of integration. Analytical expressions for $V_1(r)$ and $V_2(r)$ in terms of modified Bessel functions $I_1(\Gamma r)$ and $K_1(\Gamma r)$ where $\Gamma = \sqrt{i\sigma}$, have been derived by Carmi and Tustaniwskyj [16] with

$$V_1(r) - iV_2(r) = \frac{1}{\Delta}\left[K_1(\Gamma r_2)I_1(\Gamma r) - I_1(\Gamma r_2)K_1(\Gamma r)\right] + \frac{\varepsilon}{\eta\Delta}\left[K_1(\Gamma r)I_1(\Gamma r_1) - I_1(\Gamma r)K_1(\Gamma r_1)\right],$$

where

$$\Delta = K_1(\Gamma r_2)I_1(\Gamma r_1) - I_1(\Gamma r_2)K_1(\Gamma r_1).$$

The real and imaginary parts of this expression have been computed numerically and compared to direct numerical calculations of $V_1(r)$ and $V_2(r)$ showing an excellent agreement up to sixth digit. Asymptotic expansions of these expressions up to first order in the gap size δ were proposed by Ern [11,12]. As demonstrated in the appendix, first order corrections to the narrow gap approximation may be retrieved without mention to Bessel functions, by re-writing the base flow as $V_B = \mathcal{V}(r,t)/r^{1/2}$ and neglecting terms of order δ^2 when solving for $\mathcal{V}(r,t)$. We have drawn attention in the appendix to the questionable accuracy of the stability results obtained when using this approximation, in particular for $\varepsilon = 1$. To avoid these problems the stability analysis was always performed for a numerical velocity profile of the base flow.

Once the base flow is known, its linear stability with respect to axisymmetric disturbances is considered. The assumption of axisymmetrical modes of instability is justified for the in-phase configuration where they are the only patterns observed in experiments [6,8]. It is more questionable for the out-of-phase configuration where spiral-like non-axisymmetric patterns have been observed at high modulation frequencies [8]. When the two cylinders are counter-rotating at a uniform velocity, the threshold for the non-axisymmetric mode ($Ta_c = 65.4$) is very close to that of the axisymmetric mode ($Ta_c = 68.3$) and it is expected that the difference between the threshold values remains small when considering pulsed flows.

In the perturbed state, the velocity and pressure fields are written as the sum of a base state $(0, V_B, 0, P_B)$ and a perturbation field

$$(\mathbf{u}, p) = \big[u(r,t), v(r,t), w(r,t), p(r,t)\big] \exp(iqz),$$

where q is the wave number in the axial direction. The evolution equations for the amplitudes of the velocity components u, v, w and the pressure p are the dimensionless Navier–Stokes equations in the reference frame rotating at the angular velocity Ω_m, linearized around the basic state:

$$\frac{\partial u}{\partial t} - 2Re\left(\frac{V_B}{r} + Ro\right)v + Dp = DD_*u - q^2u, \tag{3}$$

$$\frac{\partial v}{\partial t} + Re(D_*V_B + 2Ro)u = DD_*v - q^2v, \tag{4}$$

$$\frac{\partial w}{\partial t} + iqp = D_*Dw - q^2w, \tag{5}$$

$$Du + \frac{u}{r} + iqw = 0, \tag{6}$$

with the boundary conditions $u = v = w = 0$ at $r_1 = \eta/(1-\eta)$ and $r_2 = 1/(1-\eta)$. The stability of the system is found to be governed by the Reynolds number $Re = \Omega_0 R_1 d/\nu$, the rotation number $Ro = \Omega_m d/\Omega_0 R_1$ and the frequency parameter σ. The rotation rate $\widehat{Ro} = \Omega_m/\Omega_0$ is also introduced and two different orders of magnitude which are of particular interest will be considered in Sections 4.1 and 4.2. Different notations can be found in the literature, for example in [12,14], where the set of parameters $(Ro, \widetilde{Ro})$ stands respectively for the present notations $(\widehat{Ro}, Ro)$, which are consistent with [11,13].

The system of partial differential equations (3)–(6) with time-periodic coefficients is solved by applying Floquet theory. Each of the perturbed quantities can be written in the form

$$\exp(\lambda\tau)\chi(r,\tau),$$

in which $\chi(r,\tau)$ is a periodic function in the time variable $\tau = \sigma t$ with the same period 2π as $V_B(r,\tau)$ and λ is complex equal to $\lambda_r + i\lambda_i$, λ_r is the growth rate and λ_i is a second frequency associated with quasi-periodic motion of the system. For the condition of neutral stability ($\lambda_r = 0$) and when the time-periodic part of the solution is represented by a truncated Fourier series in time, the perturbed quantities are sought as

$$\{u, v, w, p\} = \exp(i\lambda_i\tau) \sum_{n=-N}^{n=N} \{u_n(r), v_n(r), w_n(r), p_n(r)\} \exp in\tau. \tag{7}$$

The invariance of equations (3)–(6) under the combined operation of changing q in $-q$ and the complex-conjugate operation imposes restriction on the Floquet form of solution. As the real and the imaginary parts of the equations are independent, a solution can always be expressed in real form which is only possible if either $\lambda_i = 0$ (synchronous solutions) or $\lambda_i = 1/2$ (subharmonic solutions). For a particular class of temporally modulated systems (shear-induced modulation), Or [17] has been able to provide an argument for the non-existence of subharmonic solutions. In contrast, convection problems involving modulation of the thermal gradient or gravitational accceleration [18] and Taylor–Couette flow with oscillation of the outer cylinder [9] contain subharmonic as well as synchronous solutions. Though the existence of a subharmonic response cannot be definitely excluded in our problem, we have not considered this possibility on the ground that there is no experimental evidence for it. Upon substituting (7) with $\lambda_i = 0$ into the set of equations (3)–(6) leads to a system of differential equations for $u_n(r), v_n(r), w_n(r), p_n(r)$ which has been solved numerically following a method already described in [6]. A set of independent solutions satisfying the boundary conditions at $r_1 = \eta/(1-\eta)$ is constructed by a fourth-order Runge–Kutta numerical scheme with a step size ranging between 0.02 and 0.01. A linear combination of these solutions satisfying the boundary conditions at the other extreme $r_2 = 1/(1-\eta)$ leads to an homogeneous algebraic system for the coefficients of the combination. Then the condition of solvability of the system is the vanishing of the determinant which defines a dispersion relation $\Delta(\sigma, Re, q, Ro) = 0$ relating all the parameters of the problem. For the results presented here, the value of N ranged from 12 to 24 depending on frequency and rotation number. Low-frequency and high-rotation calculations require a greater number of Fourier modes in time.

3. Results for no mean rotation $Ro = 0$

We first pay attention to configurations for which there is no mean angular velocity, $\Omega_m = 0$, and then compare theoretical results to available experimental findings.

For $\varepsilon = 1$ (in-phase oscillations of the two cylinders), two configurations which correspond to $\eta = 0.9$ [6] and $\eta = 0.8$ [8] have been considered. To facilitate the comparison with previous theoretical and experimental results, we shall use the Taylor number $Ta = Re\,\delta^{1/2}$ and $\gamma = (\sigma/2)^{1/2}$ as the governing parameters of the system. It is worth noticing that γ is the ratio of two lengths, the gap width d and the thickness of the Stokes boundary layer $(2\nu/\omega)^{1/2}$. When looking for analytical expressions of the velocity profile, γ appears as a natural parameter through the expression $\Gamma = \sqrt{i\sigma} = \gamma(1+i)$ (see Section 2 and Appendix).

Evolution of the critical Taylor number as a function of γ is shown in *figure 1* for $\eta = 0.9$ and $\eta = 0.8$. Three curves which correspond respectively to the finite gap (solid lines with superimposed circles or squares) and the former small gap approximation (dashed line) [6] have been drawn. As one can notice, results from the finite gap calculations reproduce qualitatively the behavior obtained in the small gap approximation. Now concentrating on the difference, we first mention that considering a finite gap size enhances the stability of the system as for steady flows. The common features are the existence of a maximum of instability around $\gamma_0 = 2$ and the restabilization of the flow for high and low frequencies. For the two values of the gap size parameter

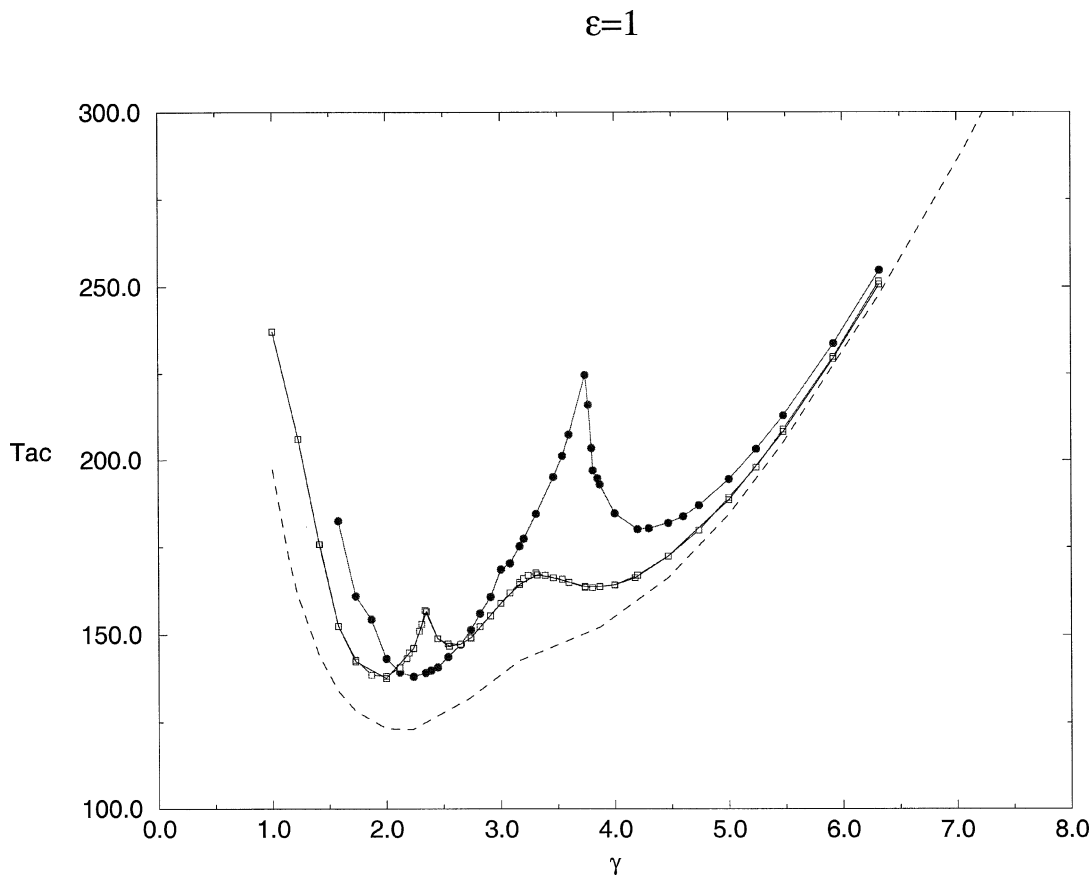

Figure 1. Critical Taylor number Ta_c versus the frequency parameter γ for in-phase oscillating cylinders ($\varepsilon = 1$) and a zero mean rotation ($Ro = 0$). Circles: $\eta = 0.8$; squares: $\eta = 0.9$. The dashed line is for the results obtained by Aouidef et al. [6] in the small gap approximation.

considered here, the critical Taylor number admits a minimum value which is nearly the same $Ta_c \approx 138$, higher than the minimum value found in the narrow gap approximation and in better agreement with previous experimental results [6,8]. The curves in *figure 1* are close to each other in the high frequency regime where it is known that the critical Taylor number obeys the asymptotic law $Ta_c \propto \gamma^{3/2}$ [6]. The difference becomes more pronounced as the frequency lowers and particularly for $\gamma \leqslant 4.5$. The present results obtained for a finite value of the gap reveal that the stability curves are not continuous but consist of two branches intersecting respectively at $\gamma = 3.75$ for $\eta = 0.8$ and $\gamma = 2.34$ for $\eta = 0.9$. This particular structure is accompanied by an abrupt change in the critical wave number as shown respectively in *figure 2(a)* for $\eta = 0.8$ and in *figure 2(b)* for $\eta = 0.9$. Though there are differences in the curves $q_c(\gamma)$ according to the value of η, a common behaviour is shared in the high frequency range where the critical wavenumber varies according to the asymptotic law $q_c \propto \gamma$ [6]. For $\eta = 0.8$, deviations from this law arise as soon as the value $\gamma = 4.2$ is reached, which coincides with a local minimum in the curve $Ta_c(\gamma)$ also present, even if less pronounced, in the experimental curve [8]. Then, for $\gamma = 3.75$ there is a jump in the curve $q_c(\gamma)$ which corresponds to the intersection of the two stability branches in the $Ta_c(\gamma)$ diagram. For $\eta = 0.9$, the value $\gamma = 3.5$ corresponds to a minimum of q_c and to a shouldering in the curve $Ta_c(\gamma)$ which was already detected in the narrow gap calculations as well as in experiments [6]. For the lower value of $\gamma = 2.34$ we finally observed a jump in the value of q_c which is similarly associated to the intersection of the two stability branches in the $Ta_c(\gamma)$ diagram.

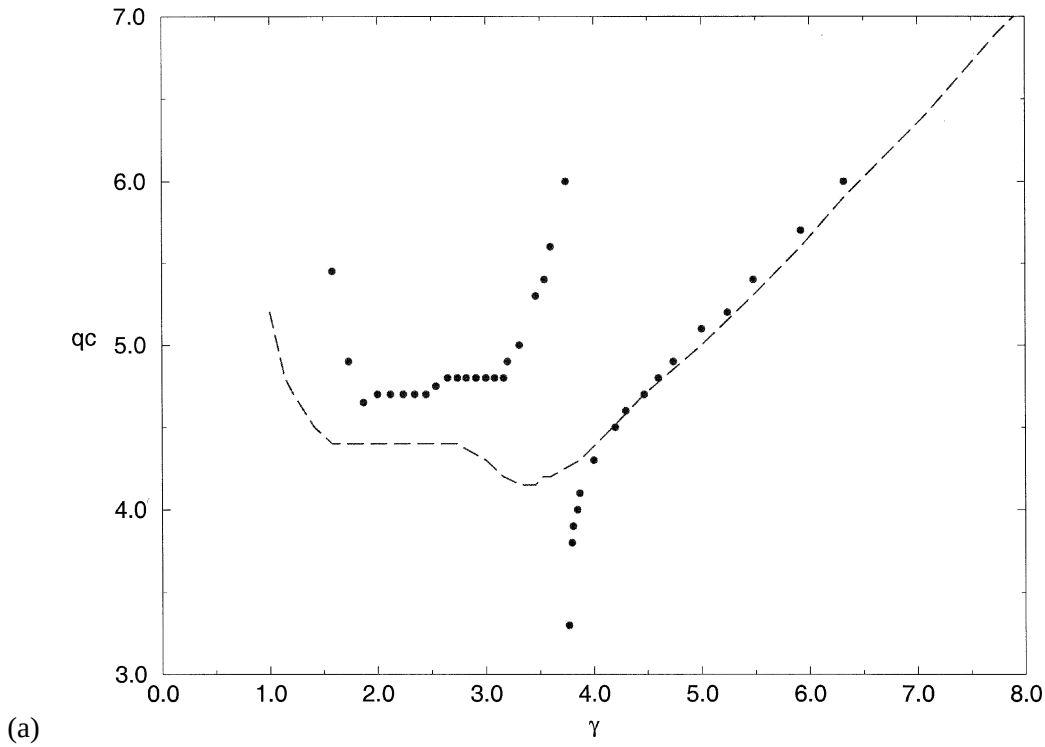

(a)

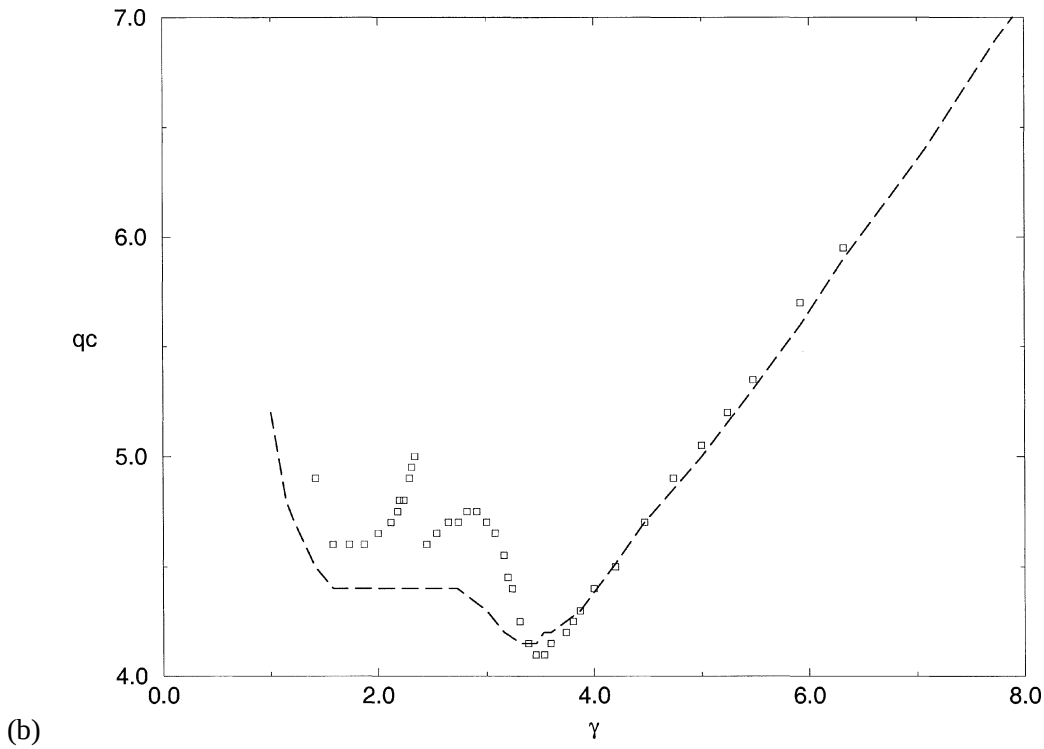

(b)

Figure 2. Critical wavenumber q_c versus γ for the same parameters as *figure 1* ($\varepsilon = 1$, $Ro = 0$). (a) Circles: $\eta = 0.8$; (b) squares: $\eta = 0.9$. The dashed line is for the results obtained by Aouidef et al. [6] in the small gap approximation.

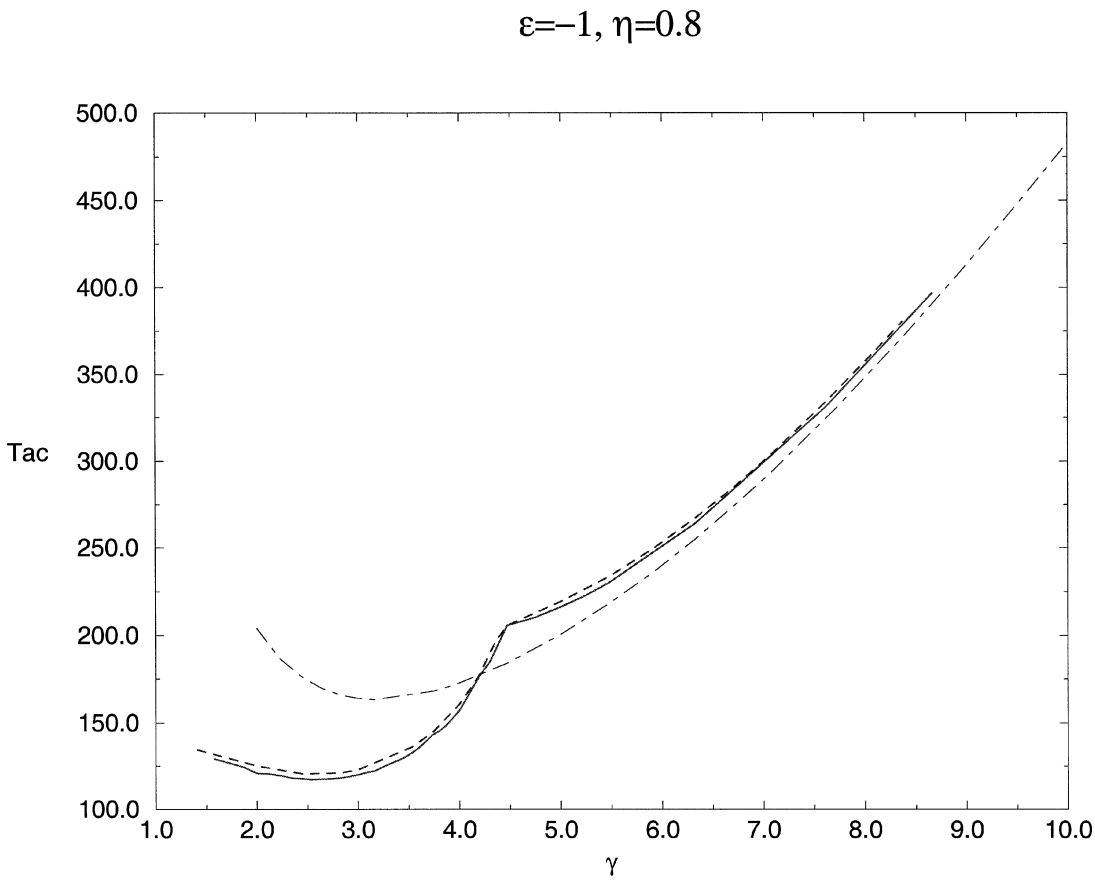

Figure 3. Critical Taylor number Ta_c versus the frequency parameter γ for out-of-phase oscillating cylinders ($\varepsilon = -1$) and $\eta = 0.8$. Different approximations of the radial velocity profiles have been used. Solid line: numerical profile; dot-dashed line: small gap approximation (Tennakoon et al. [8]); dashed line: first order corrections to the small gap approximation are taken into account.

The second configuration we considered is when the cylinders are subject to out-of-phase oscillations ($\varepsilon = -1$) and with $\eta = 0.8$ [8]. In *figures 3* and *4* are reported evolutions of the critical Taylor number and wavenumber in terms of the frequency number γ. The dot-dashed line represents the theoretical results in the small gap approximation of [8], the solid line is the present investigation when using the numerical velocity profile and the dashed line when using the approximate velocity profile derived in the Appendix. For high frequencies, a restabilization of the flow is revealed and the critical values are found to obey asymptotically the laws $Ta_c \propto \gamma^{3/2}$ and $q_c \propto \gamma$. For low frequencies, we recover a much better agreement with experiments than we did in our previous study [8] when using a narrow gap approximation. In particular, for the lowest values of γ considered the critical Taylor number slightly increases above its minimum value $Ta_c^{\min} = 117$ reached for $\gamma = 2.5$, while the experimental results show that for $\gamma < 3$ the critical Taylor number keeps a nearly constant value $Ta_c \approx 100$. A second important point is that the marginal stability curves were found to exhibit two distinct branches with two local minima leading then to improve the agreement for the evolution of the critical wavenumber in terms of the frequency γ as shown in *figure 4*. For $\gamma \approx 4.3$ there is an exchange of stability between the left and the right branches of the neutral curve $Ta(q)$ which results in a discontinuity in the curve $q_c(\gamma)$ and a change in the slope of the curve $Ta_c(\gamma)$ in agreement with the experimental results plotted in figure 12 of reference [8].

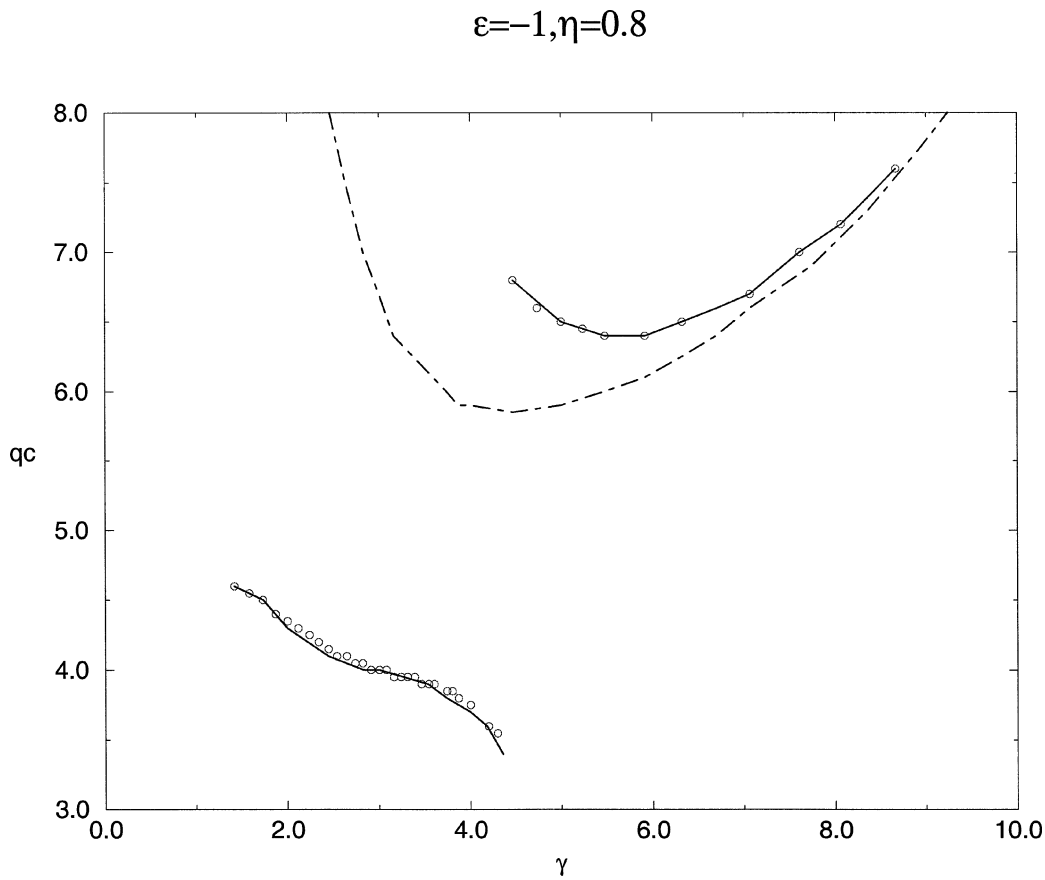

Figure 4. Critical wavenumber q_c versus γ for the same parameters as *figure 3* ($\varepsilon = -1$ and $\eta = 0.8$). Circles: numerical profile; dot-dashed line: small gap approximation (Tennakoon et al. [8]); solid line: first order corrections to the small gap approximation are taken into account.

To conclude, it is worth noticing that our finite gap results differs from those obtained previously by Carmi and Tustaniwskyj [16] for a gap size $\delta = 0.444$ ($\eta \approx 0.7$). For $\varepsilon = +1$ they found a minimum value of Ta_c much lower than ours and for $\varepsilon = -1$ they found a restabilization of the flow when $\gamma \to 0$ in contradiction with the present results and experimental findings [8]. Disagreements with the results of Carmi and Tustaniwskyj [16] were already pointed out in other studies [9,19] concerned with a different configuration (steady rotation of the inner cylinder and sinusoidal oscillation of the outer cylinder about a zero mean). It was suggested that insufficient temporal resolution in their computations was responsible for the discrepancy, especially in the low frequency range.

4. Results for $Ro \neq 0$

In this section we shall concentrate on the configuration corresponding to $\varepsilon = 1$ and $\eta = 0.9$ for which the experimental procedure described in reference [11] provided results that can be directly compared with our theoretical findings. Experiments have been conducted at different values of the frequency and for each value the critical Taylor number is reported as a function of the rotation number. We shall mention that a different procedure has been implemented in reference [8] where experiments were performed at a fixed value of the mean rotation $\Omega_m = 1.26$ rad/sec while Ω_0 was varied until its threshold value for instability. In this case, the

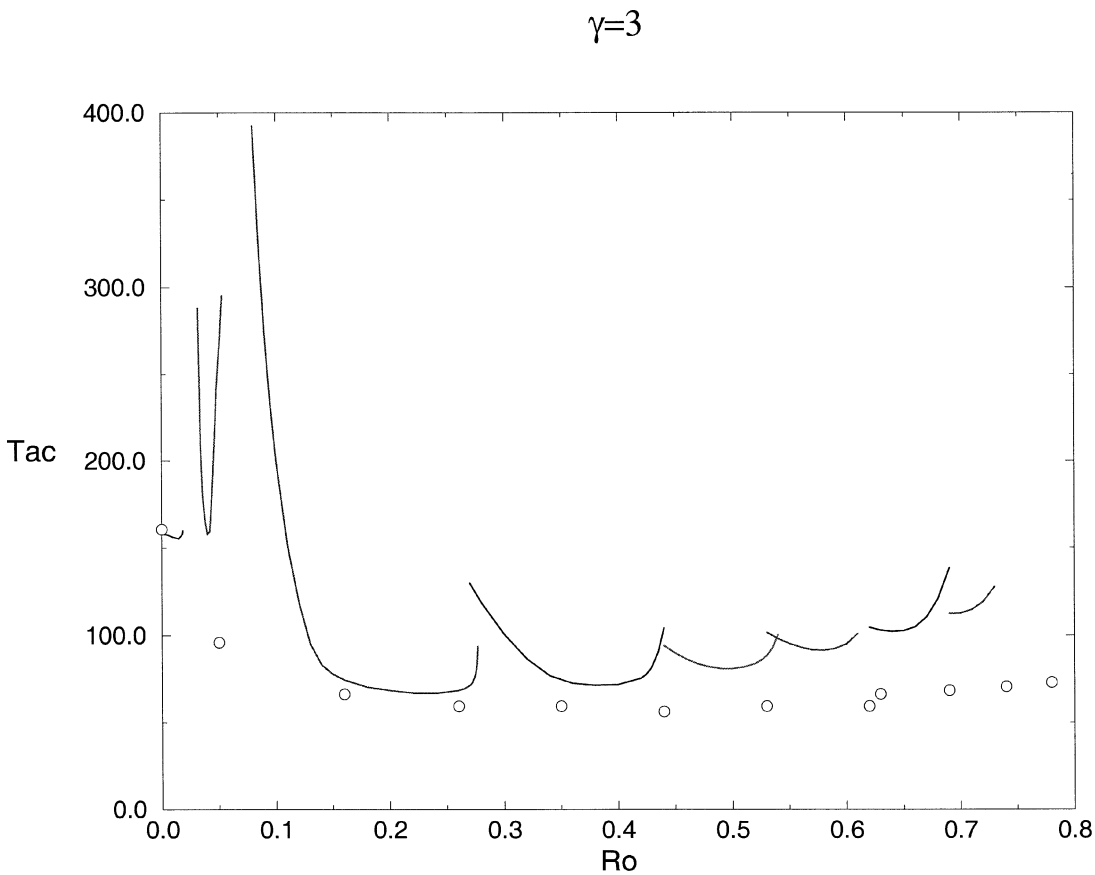

Figure 5. Critical Taylor number Ta_c versus the rotation parameter Ro for in-phase oscillations ($\varepsilon = 1$) at the frequency number $\gamma = 3$. The circles are the experimental results of Ern [11].

Taylor number Ta and the rotation rate $\widehat{Ro}$ are not independent parameters and the experimental results show the critical value of the modified Taylor number $\widetilde{Ta}_c = Ta_c(1 + \widehat{Ro}^2)^{1/2}$ as a function of γ. This formulation is less suitable for direct comparison with our theoretical results since it focuses on the variations of $\widetilde{Ta}_c$ versus the frequency parameter γ. We prefer to consider only two values of the frequency and examine the influence of the rotation number on Ta_c.

Our results presented in *figures 5* and *7* show the critical value of Ta_c as a function of Ro for two values of the frequency parameter $\gamma = 3$ and $\gamma = 4.5$. The corresponding values of the critical wavenumber are shown in *figures 6* and *8*. The results are given for $Ro \leqslant 1.0$ since for larger values of Ro the computations which require more and more Fourier modes converge very slowly. This difficulty also reported for $Ro = 0$ when $\gamma \leqslant 1$, arises when the steady component of the flow dominates, either because the frequency goes to zero or the mean rotation increases.

Considering the curves $Ta_c(Ro)$ we first notice that they are not continuous and consist in several branches. The curves in *figures 5* and *7* both exhibit the same qualitative features, except for very low values of the rotation number. When $\gamma = 4.5$, the critical Taylor number starts with the value $Ta_c = 174$ for $Ro = 0$, then sharply increases when Ro is increased. When $\gamma = 3$, the critical Taylor number value which is $Ta_c = 158$ for $Ro = 0$, remains nearly constant on a very short range of Ro values. This results from the topology of the neutral curves $Ta(q)$ that undergo deformations when Ro increases as shown in *figure 9* when $\gamma = 3$. For very

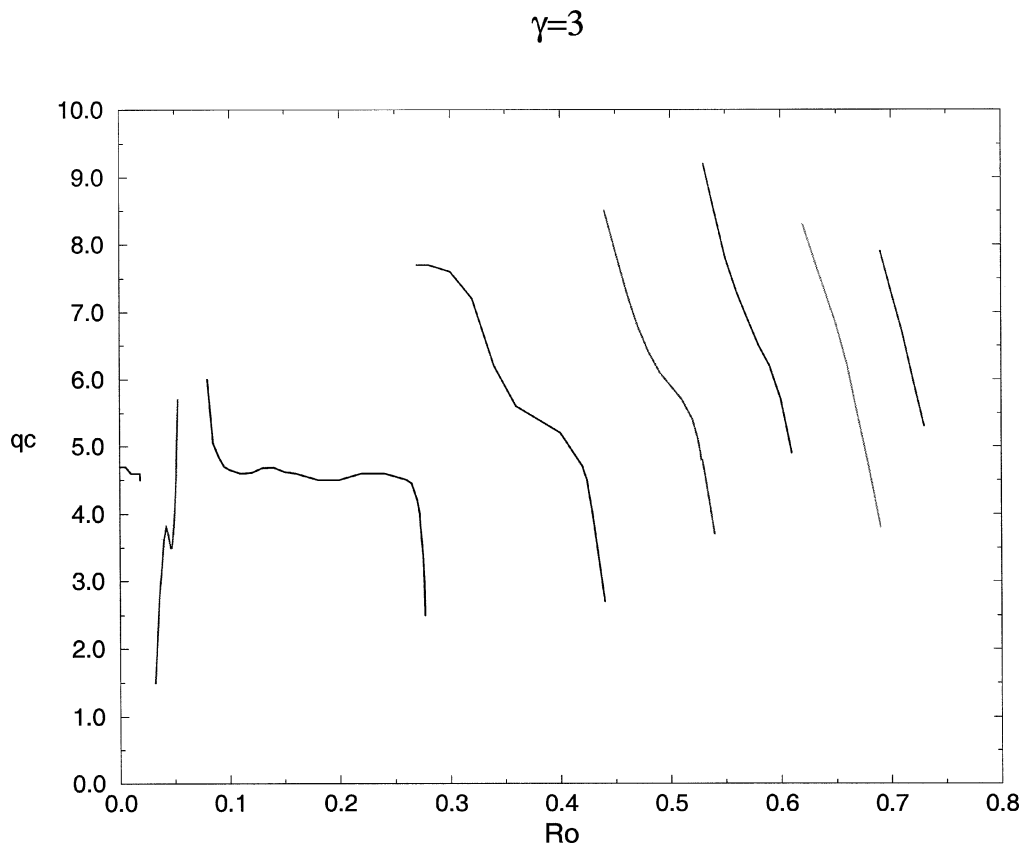

Figure 6. Critical wave number q_c versus the rotation parameter *Ro* for in-phase oscillations ($\varepsilon = 1$) at the frequency number $\gamma = 3$.

low values of *Ro*, and near the critical point occuring for $q \approx 4.5$, the neutral curves have a parabolic shape that becomes a closed loop with increasing *Ro*. Then the size of the loop reduces until finally it shrinks for a value of $Ro \approx 0.0185$. Similar ring-shaped neutral curves enclosing unstable islands have also been reported by Or [17] when studying instability in a horizontal liquid layer on an oscillating plane. For larger values of *Ro*, the critical point is on a higher neutral curve and its evolution gives rise to a secondary branch in the $Ta_c(Ro)$ diagram with a local minimum $Ta_c = 158$ at $Ro = 0.04$. A secondary branch also exists when $\gamma = 4.5$, with a local minimum $Ta_c = 139$ at $Ro = 0.055$, which ends up abruptly following the same scenario as the one described in *figure 9*.

For still higher but moderate values of *Ro*, the critical Taylor number lies on a third disconnected branch and it lowers abruptly to reach a minimum value $Ta_c \approx 67$ located respectively at $Ro = 0.24$ for $\gamma = 3$ and at $Ro = 0.3$ for $\gamma = 4.5$. In the set of experiments to which we refer [11], a maximum of destabilization was reported for values of the rotation number in the range $0.3 \leqslant Ro \leqslant 0.6$ corresponding to the minimum values of the Taylor number $Ta_c^{\min} = 59$ for $\gamma = 3$ and $Ta_c^{\min} = 67$ for $\gamma = 4.5$ consistent with our theoretical results.

For higher values of *Ro*, the critical Taylor number increases in agreement with experimental data recorded up to $Ro = 1.4$ [11]. An asymptotic formula giving the critical Taylor number in the high rotation regime has been derived for steady flows [14] which predicts restabilization for $Ro > 3$ in the case of a Poiseuille profile. This result is not directly transposable to time periodic flows subject to rotation for which the appropriate asymptotic analysis will be presented in Section 4.1 for the two limiting cases of low and high modulation frequency.

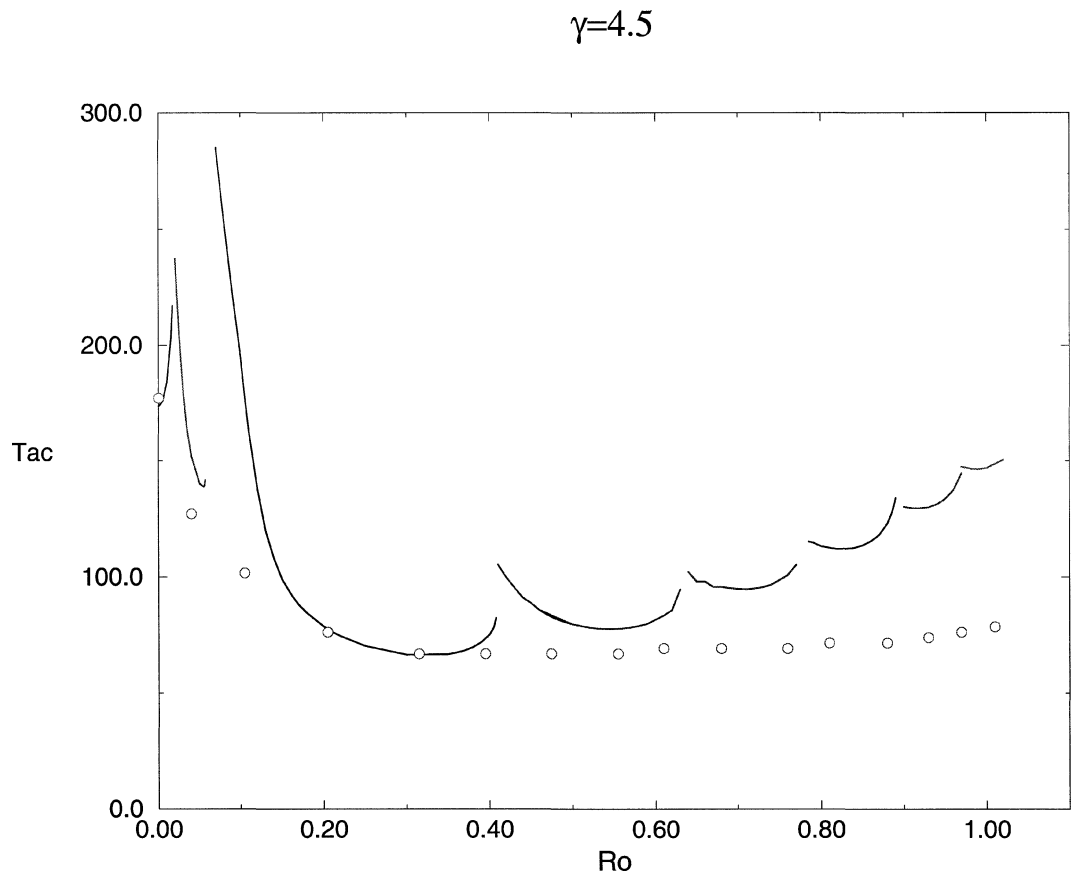

Figure 7. Critical Taylor number Ta_c versus the rotation parameter *Ro* for in-phase oscillations ($\varepsilon = 1$) at the frequency number $\gamma = 4.5$. The circles are the experimental results of Ern [11].

The restabilization of the flow near $Ro \approx 0.1$ was not easy to detect in experiments mainly because only one value of *Ro* was considered in the range $0 < Ro < 0.1$. The enhancement of stability is reminiscent of a similar phenomenon already mentioned for steady flows under rotation [13,14] and attributed to the cancellation of Coriolis and centrifugal effects. It was shown to occur for small and negative values of the rotation number $Ro = -\delta$ [15]. In the present study the gap size is $\delta = 0.112$ and since the direction of rotation is not a relevant parameter in the case of a time periodic base flow, it appears that the formula $|Ro| \approx \delta$ still provides a good approximation for the location of the point at which Coriolis and centrifugal effects cancel each other. A more rigorous treatment based on the generalization to time-periodic flows of an argument first introduced by Mutabazi et al. [14] for steady flows has been reported in Section 4.2.

4.1. High rotation regime and small gap approximation

We shall use the small gap approximation and write the radial variable as $r = \delta^{-1} + x$ with $0 \leqslant x \leqslant 1$. Terms of order δ are neglected except in the centrifugal term and the perturbations equations now take the form

$$(\sigma\partial_\tau - \mathcal{L})\mathcal{L}u + 2q^2 Ta\big(V_B + \widehat{Ro}\big)v = 0, \tag{8}$$

$$(\sigma\partial_\tau - \mathcal{L})v + Ta\big(DV_B + 2\delta\widehat{Ro}\big)u = 0, \tag{9}$$

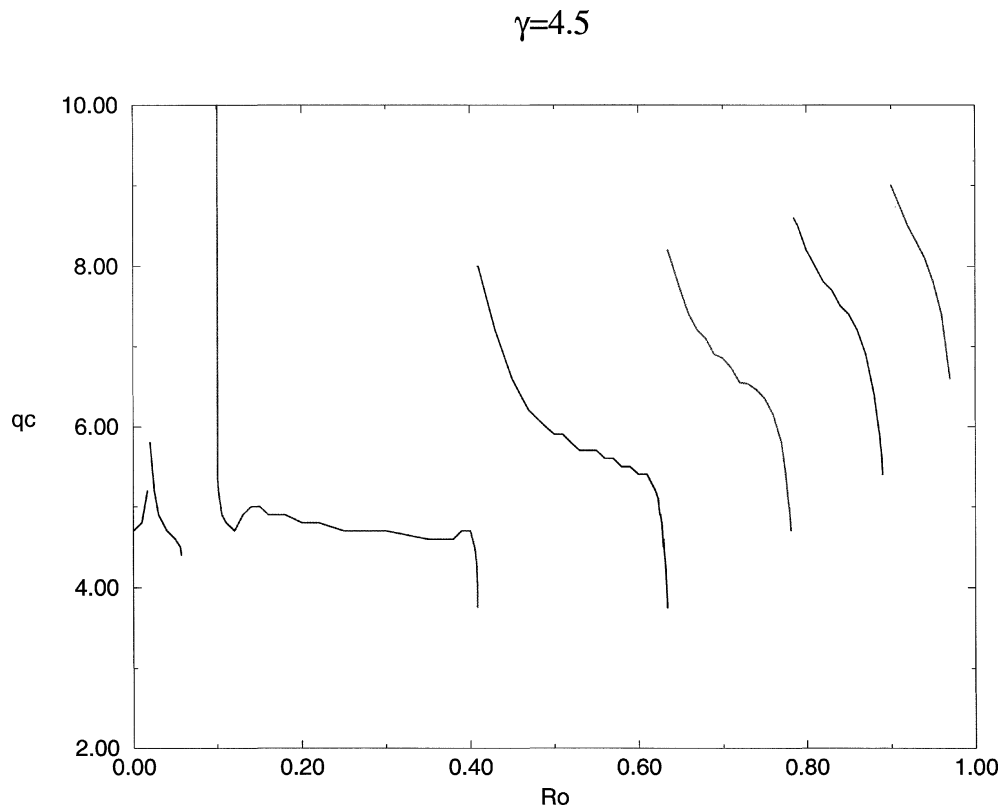

Figure 8. Critical wave number q_c versus the rotation parameter Ro for in-phase oscillations ($\varepsilon = 1$) at the frequency number $\gamma = 4.5$.

where $\mathcal{L} = \partial^2/\partial x^2 - q^2$. We shall consider high rotation rate such that $\delta\widehat{Ro} \approx \mathcal{O}(1)$ and examine successively the low and high frequency regimes.

In the low frequency regime, the quasi-static approximation can be used and the above equations reduce to

$$\mathcal{L}^2 u + 2q^2 Ta\widehat{Ro} = 0, \tag{10}$$

$$\mathcal{L}v + Ta\big(DV_B + 2\delta\widehat{Ro}\big)u = 0. \tag{11}$$

The inviscid Rayleigh criterion for stability requires that the sign of the discriminant

$$\phi(x,\tau) = \widehat{Ro}\big(DV_B + 2\delta\widehat{Ro}\big),$$

must be negative for instability to set in [14]. It is known [6] that for $\gamma \to 0$, the derivative of the base flow velocity expands as

$$DV_B = \gamma^2(1-2x)\sin\tau + \mathcal{O}\big(\gamma^4\big).$$

As the Rayleigh discriminant is invariant in the transformation $(\widehat{Ro},\tau) \to (-\widehat{Ro},\tau+\pi)$ only positive values of $\widehat{Ro}$ will be considered. For positive values of $\sin\tau$, the condition for instability gives for x

$$x_0 = \frac{1}{2} + \frac{\widehat{Ro}\,\delta}{\gamma^2\sin\tau} \leqslant x \leqslant 1,$$

which defines an unstable fluid layer located near the outer cylinder whose extension is $1 - x_0$.

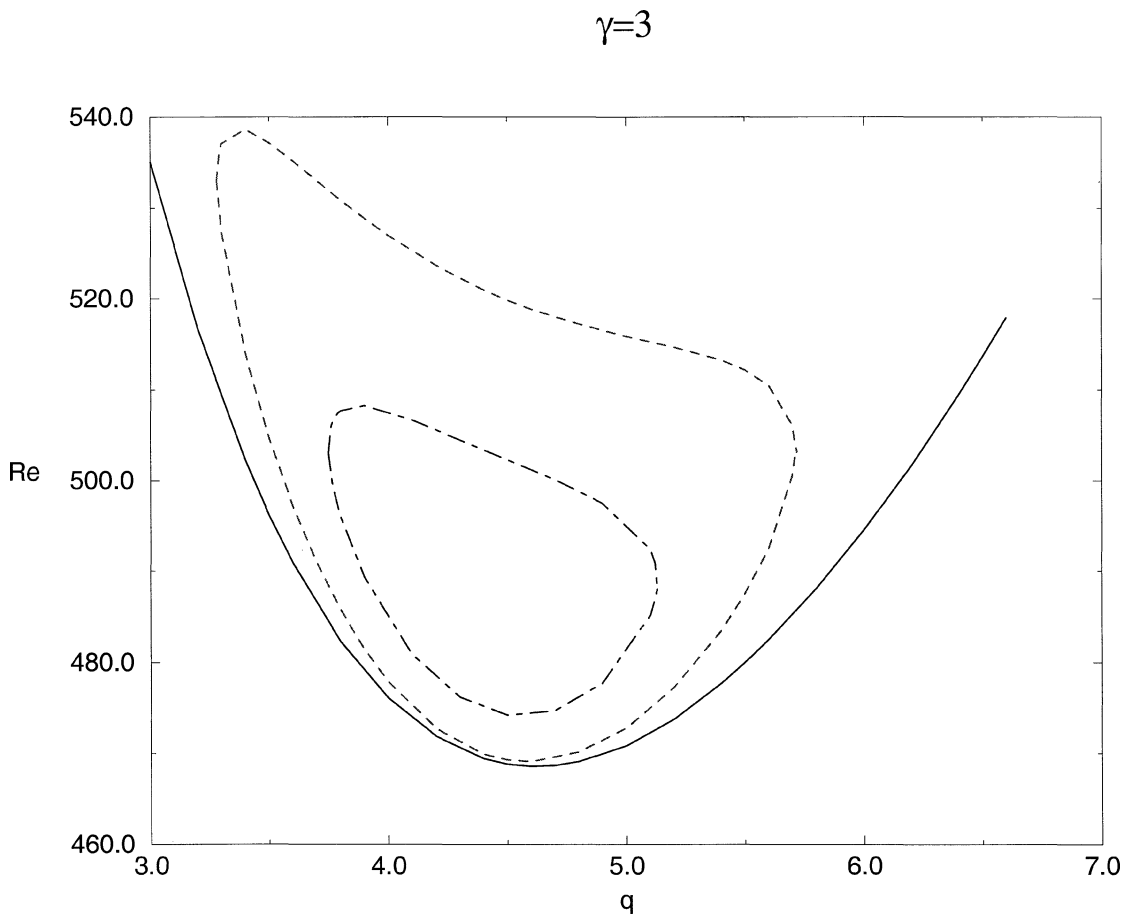

Figure 9. Evolution of the neutral curves (Reynolds number *Re* versus wave number q) for the fixed set of parameters: $\gamma = 3$, $\eta = 0.9$ and $\varepsilon = 1$, when the rotation number *Ro* is varied. Solid line: $Ro = 0.01$; dashed line: $Ro = 0.017$; dot-dashed line: $Ro = 0.018$.

For negative values of $\sin\tau$, the unstable layer lies near the inner cylinder

$$0 \leqslant x \leqslant x_0 = \frac{1}{2} + \frac{\widehat{Ro}\,\delta}{\gamma^2 \sin\tau}.$$

Thus, whatever the sign of $\sin\tau$, the extension of the unstable layer decreases with increasing $\widehat{Ro}$ until it vanishes as $\delta\widehat{Ro} \to \gamma^2|\sin\tau|/2$. The asymptotic behavior in the stability diagram $(Ta_c, \delta\widehat{Ro})$ may be found by using the dynamical similarity of equations (10)–(11) with Taylor–Couette system equations [14,15]. Therefore, with the correspondence

$$1 - \mu \Leftrightarrow \left(\frac{1}{2} - \frac{\widehat{Ro}\,\delta}{\gamma^2|\sin\tau|}\right)^{-1},$$

$$T \Leftrightarrow 4\gamma^2 {Ta_c}^2 \widehat{Ro}\left(\frac{1}{2} - \frac{\widehat{Ro}\,\delta}{\gamma^2|\sin\tau|}\right),$$

where μ is the rotation ratio of the cylinders and $T = 1181(1-\mu)^4$ is the Taylor number in the Taylor–Couette system as given by Chandrasekhar [15] for large negative values of μ, one obtains the following asymptotic

relation

$$Ta_c = \frac{97.2}{\gamma \widehat{Ro}^{1/2}} \left(1 - \frac{2\widehat{Ro}\,\delta}{\gamma^2}\right)^{-5/2}. \tag{12}$$

In the high frequency regime the choice of d as the length scale is not appropriate because the base flow velocity takes appreciable values in the inner and outer Stokes boundary layers of size d/γ. Therefore it is convenient to make the change of variables:

$$x = \gamma^{-1}\tilde{x} \quad \text{and} \quad q = \gamma \tilde{q}.$$

Moreover, in the expression $DV_B = DV_1 \cos\tau + DV_2 \sin\tau$, the spatial distributions $DV_1(x)$ and $DV_2(x)$ reach their maximum values on $x = 0$ and $x = 1$ with $DV_1(0) \approx -\gamma$ and $DV_2(0) \approx \gamma$ when $\gamma \gg 1$. Therefore, according to the Rayleigh criterion the maximum of instability will arise when either $\cos\tau = 1$ or $\sin\tau = -1$, with the corresponding value of the discriminant: $\phi = \widehat{Ro}(2\widehat{Ro}\,\delta - \gamma)$. A balance of the various terms in equations (8)–(9) gives the relationships $\gamma^2 u \sim Ta_c \widehat{Ro}\, v$ and $\gamma^2 v \sim Ta_c(2\widehat{Ro}\,\delta - \gamma)u$ which are simultaneously satisfied provided that

$$Ta_c \sim \frac{\gamma^{3/2}}{\widehat{Ro}^{1/2}(1 - 2\widehat{Ro}\,\delta/\gamma)^{1/2}}. \tag{13}$$

In the high rotation range, the Coriolis force restabilizes the flow and leads to the Taylor–Proudman two-dimensional regime as in the case of steady flows [14]. The asymptotic value of Ro^+ at which there is a complete restabilization of the flow is given by $Ro^+ = \gamma^2/2$ for low frequency values (equation (12)) and by $Ro^+ = \gamma/2$ for high frequencies (equation (13)).

4.2. Low rotation regime and small gap approximation

In the small gap approximation for moderate values of the rotation number $\widehat{Ro} \sim \mathcal{O}(1)$, the Rayleigh discriminant becomes $\phi(x,\tau) = (\widehat{Ro} + V_B)DV_B$. Using the asymptotic expansions of V_B and DV_B in the low frequency range ($\gamma \to 1$), Ern [11] analyzed the sign of the discriminant

$$\phi(x,\tau) = \left[\widehat{Ro} + \cos\tau + \gamma^2 x(1-x)\sin\tau\right]\gamma^2(1-2x)\sin\tau.$$

Following a procedure first introduced by Aouidef et al. [6] when there is no rotation, Ern remarked that at time τ_0 such as $\widehat{Ro} + \cos\tau_0 = 0$, or equivalently $\sin\tau_0 = \pm(1 - \widehat{Ro}^2)^{1/2}$, the discriminant becomes identical to the one associated to the Dean problem (instability of Poiseuille flow in a curved channel) with the correspondence

$$De_c = Ta_c\gamma^2\left(1 - \widehat{Ro}^2\right)^{1/2},$$

where $De_c = 215$ is the critical value of the Dean number. This expression shows that $Ta_c(\tau_0)$ diverges when $\widehat{Ro} \to 1$ ($Ro \to \delta$). As a complement to Ern's analysis we have found other values of the time leading to an enhancement of the instantaneous critical Taylor number. This is due to the competition between the centrifugal force and the Coriolis force both acting as the destabilizing mechanisms in the system. It is worth selecting τ_0 such as $\cos\tau_0 = 0$ and $\sin\tau_0 = -1$, so that the discriminant reads

$$\phi(x,\tau) = \left[\gamma^2 x(1-x) - \widehat{Ro}\right](1-2x)\gamma^2.$$

As noticed by Mutabazi et al. [14] in their study of rotation effects on centrifugally driven instabilities in steady flows, the above disciminant should be considered as the Rayleigh discriminant for the equivalent velocity profile $V_e = \gamma^2 x(1-x) - \widehat{Ro}$. For $\widehat{Ro} \leqslant 0$, the flow consists of two layers, with the one close to the outer cylinder centrifugally unstable even when $\widehat{Ro} = 0$. Negative values of $\widehat{Ro}$ will then enhance the effect of the centrifugal force. For $\widehat{Ro} \geqslant \gamma^2/4$, the flow also consists of two layers, with the one close to the inner cylinder unstable to rotation-induced perturbations. For intermediate values $\widehat{Ro} \in [0, \gamma^2/4]$, there are two potentially unstable layers alternating with two stable layers. The rotation annihilates the effect of the curvature when the net flux of the equivalent velocity across the gap is zero $\int_0^1 V_e\,dx = 0$; this happens when $\widehat{Ro} = \gamma^2/6$. This argument can be repeated without the low frequency assumption and for any values of the time. In the general case, the zero flux condition expresses as

$$\cos\tau_0 \int_0^1 V_1(x)\,dx + \sin\tau_0 \int_0^1 V_2(x)\,dx + \widehat{Ro} = 0,$$

which, after integration, gives the value of $\widehat{Ro}$ at which Coriolis and centrifugal effects cancel each other:

$$\widehat{Ro} + \frac{(\sinh\gamma + \sin\gamma)\cos\tau_0 + (\sinh\gamma - \sin\gamma)\sin\tau_0}{\gamma(\cosh\gamma + \cos\gamma)} = 0.$$

For $\gamma = 3$ and $\gamma = 4.5$ there is no experimental evidence of restabilisation of the flow in the low rotation regime but for a lower value $\gamma = 1$ [11,20], no critical value of the Taylor number was found in the range $0.05 < Ro < 0.1$ which can be attributed to the cancellation of the two destabilizing mechanisms.

5. Conclusion

The aim of this work was to present theoretical results stemmed from the linear stability analysis of pulsed flows in a Taylor–Couette geometry with the inner and outer cylinders rotating respectively at $\Omega_1(t) = \Omega_m + \Omega_0\cos(\omega t)$ and $\Omega_2(t) = \Omega_m + \varepsilon\Omega_0\cos(\omega t)$. This investigation was conducted in the finite gap formulation, with $\varepsilon = \pm 1$, for different values of the frequency parameter γ and rotation number Ro. As a first check for the reliability of our stability scheme, the situation for which there is no rotation effects ($Ro = 0$) was investigated. For $\varepsilon = +1$, the main results revealed that when one takes into account the finite gap geometry, the stability of the flow is enhanced when compared to the small gap approximation, in agreement with classical experimental and theoretical findings. For $\varepsilon = -1$, we have found a new branch of instability in the low frequency range which better fits with the existing experimental results. Moreover, a 'semi-analytical' solution was proposed as an alternative for the Bessel functions to describe the base flow when the cylinders'geometry is such that $\delta = d/R_1 \ll 1$. For the radius ratio $\eta = 0.8$, a satisfactory agreement with a fully numerical analysis was found for counter-rotating cylinders ($\varepsilon = -1$) whereas a discrepancy was revealed for co-rotating cylinders ($\varepsilon = +1$) which requires more theoretical investigations for a full understanding.

As a second set of results ($Ro \neq 0$), we paid attention to the Coriolis effects on the stability of a pulsed flow by letting the rotation number vary in the range $Ro \in [0, 1.0]$ and fixing the frequency parameter to $\gamma = 3$ and $\gamma = 4.5$ since there are available experimental data for comparaison. For both frequencies, evolution of the critical parameters versus the rotation number were reported as a discontinuous series of curves with a maximum of destabilization for $Ro = 0.3$. A general tendency towards a restabilization of the flow when $Ro \approx \delta$ as well as when Ro increases towards the upper value ($Ro = 1.0$) considered is reported. These two features are reminiscent of what is known to occur when steady flows in curved channels are subject to rotation. For highest

rotation numbers, the Coriolis force restabilizes the flow and leads to the Taylor–Proudman two-dimensional regime. For pulsed flows, the asymptotic value of Ro^+ at which there is a complete restabilization depends on the frequency parameter. It is given by $Ro^+ = \gamma^2/2$ for low frequencies and $Ro^+ = \gamma/2$ for high frequencies. In the low rotation regime ($Ro \propto \delta$) we have shown that the near cancellation of centrifugal and Coriolis effects is responsible for enhancement of stability.

The present analysis scheme allows for many configurations to be treated in terms of frequency and rotation numbers and gave satisfactory results when compared to rare, available experimental investigations. Despite the difficulties due to the rotation effects as well as the unsteadiness of the flow, more experiments would be welcome, particularly in the low rotation regime, to confirm the restabilization predicted to occur when the rotation number and the gap size are of the same order of magnitude.

Appendix

Using the transformation $V_B = \mathcal{V}(r,t)/r^{1/2}$ in equation (1), we get the following equation for $\mathcal{V}(r,t)$:

$$\frac{\partial \mathcal{V}}{\partial t} = \frac{\partial^2 \mathcal{V}}{\partial r^2} - \frac{3}{4}\frac{\mathcal{V}}{r^2}.$$

The scaling for time, distance and velocity being the same as in Section 2, the non-dimensional radial variable is now written as $r = (1+\delta x)/\delta$ where the quantity $\delta = d/R_1$ is introduced. If terms of order δ^2 are neglected, the above equation reduces to

$$\frac{\partial \mathcal{V}}{\partial t} = \frac{\partial^2 \mathcal{V}}{\partial x^2},$$

to be solved with the boundary conditions

$$\mathcal{V}(0,t) = \cos(\sigma t), \qquad \mathcal{V}(1,t) = \varepsilon(1+\delta)^{3/2}\cos(\sigma t).$$

At this stage the determination of $\mathcal{V}$ bears a close analogy with the derivation of V_B in the narrow gap approximation (Aouidef et al. [6]), the only difference being the presence of a factor $(1+\delta)^{3/2}$ in the boundary condition at $x = 1$. Therefore, the solution is sought as

$$\mathcal{V} = A(x)\cos(\sigma t) + B(x)\sin(\sigma t),$$

where

$$A(x) = F(x) + \varepsilon(1+\delta)^{3/2}G(x)$$

and $B(x) = \sigma^{-1}(\partial^2 A/\partial x^2)$. The expressions for $F(x)$ and $G(x)$ are found to be

$$F(x) = \frac{1}{2}\frac{\sinh\Gamma(1-x)}{\sinh\Gamma} + \text{c.c.},$$
$$G(x) = \frac{1}{2}\frac{\sinh\Gamma x}{\sinh\Gamma} + \text{c.c.},$$

with $\Gamma = \gamma(1+i)$ and c.c. stands for complex conjugate, thus recovering expressions identical to those obtained in [11,12] by asymptotic expansions of Bessel functions. Moreover, one can show after some algebra that the

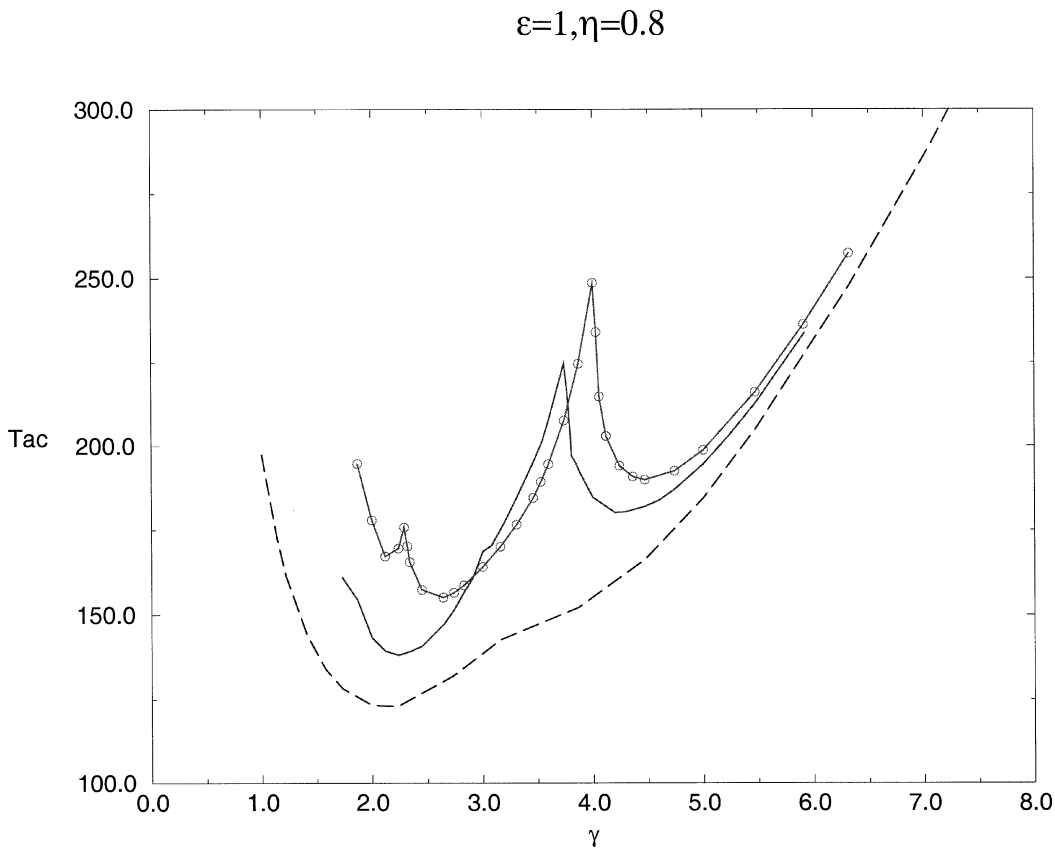

Figure 10. Comparison of the values of $Ta_c(\gamma)$ obtained when using different approximations for the radial profiles of the base flow velocity V_B ($\varepsilon = 1$). Solid line: numerical determination of the velocity profiles for $\eta = 0.8$; dashed line: small gap approximation; circles: first order corrections to the small gap approximation are taken into account.

functions $F(x)$ and $G(x)$ are related in a simple way to the radial distributions $V_1(x)$ and $V_2(x)$ which appear in the narrow gap approximation of the base flow velocity written as:

$$V_B = V_1(x)\cos(\sigma t) + V_2(x)\sin(\sigma t),$$

where the explicit forms of $V_1(x)$ and $V_2(x)$ are given in [7]. The following relations are found

$$F(x) = \frac{1}{2}\{V_1(x, \varepsilon = 1) + V_1(x, \varepsilon = -1)\},$$
$$G(x) = \frac{1}{2}\{V_1(x, \varepsilon = 1) - V_1(x, \varepsilon = -1)\}.$$

Similarly $B(x)$ can be expressed in terms of $V_2(x, \varepsilon = \pm 1)$.

Since the above derivation provides accurate values of the basic velocity profile an attempt was made to use it and the corresponding expression for $D_* V_B$ in our stability analysis for the case $Ro = 0$. For $\varepsilon = -1$, the stability curves are in close agreement whether they are obtained from the above expansion of the velocity profile or from the numerical derivation. Unexpectedly, for $\varepsilon = +1$, we calculated results which differ from those obtained when V_B is determined numerically, in particular the curves $Ta_c(\gamma)$ are shifted towards higher values (see *figure 10*). Inspection of the values of $D_* V_B$ reveals that at mid-gap the out-of-phase contribution

deduced from $B(x)$ takes small values that are overestimated if compared to their numerical values. It is the only feature worth mentioning as a possible origin of the discrepancy though it is not yet understood how it leads to enhance the stability.

This approximation for the base flow velocity was originally derived in a different way by Ern [11,12] and used in a quasi-static approach for the value $\gamma = 1$, leading to a minimum value of the instantaneous Taylor number $Ta_c \approx 200$, comparable to the value found earlier by Aouidef et al. [6] using Floquet theory and the narrow gap approximation. Extrapolation of the present finite gap results to $\gamma = 1$ suggests that a higher value of Ta_c should be expected.

Acknowledgements

We are grateful to P. Ern and J.E. Wesfreid for communicating their experimental results. The revised version of the manuscript has benefited from stimulating discussions with I. Mutabazi.

References

[1] Davis S.H., The stability of time-periodic flows, Annu. Rev. Fluid Mech. 8 (1976) 57–74.
[2] Ostrach S., Low-gravity fluid flows, Annu. Rev. Fluid Mech. 14 (1982) 313–345.
[3] Singh M.P., Sinha P.C., Aggarwal M., Flow in the entrance of the aorta, J. Fluid Mech. 87 (1978) 97–120.
[4] Faraday M., On the forms and states of fluids on vibrating elastic surfaces, Philos. T. Roy. Soc. 52 (1831) 319–340.
[5] von Kerczek C., Davis S.H., The stability of oscillatory Stokes layers, Stud. Appl. Math. LI (1972) 239–252.
[6] Aouidef A., Normand C., Stegner A., Wesfreid J.E., Centrifugal instability of pulsed flow, Phys. Fluids 11 (1994) 3665–3676.
[7] Aouidef A., Normand C., Instability of pulsed flows in a Taylor–Couette geometry, C. R. Acad. Sci. II B 322 (1996) 545–552.
[8] Tennakoon S.G.K., Andereck C.D., Aouidef A., Normand C., Pulsed flow between concentric rotating cylinders, Eur. J. Mech. B-Fluid. 16 (1997) 227–248.
[9] Murray B.T., McFadden G.B., Coriell S.R., Stabilization of Taylor–Couette flow due to time-periodic outer cylinder oscillation, Phys. Fluids A-Fluid. 2 (1990) 2147–2156.
[10] Ern P., Stegner A., Ollivier M., Wesfreid J.E., Influence de la rotation sur les instabilités hydrodynamiques, Actes du 12ème Congrès Français de Mécanique (A.U.M.), Strasbourg, 1995.
[11] Ern P., Instabilités d'écoulements périodiques en temps avec effets de courbure et de rotation, Thèse de doctorat de l'Université Paris VI, 1997.
[12] Ern P., A study on time-periodic finite-gap Taylor–Couette flows, C. R. Acad. Sci. II B 326 (1998) 727–732.
[13] Matsson O.J.E., Alfredsson P.H., Curvature- and rotation-induced instabilities in channel flow, J. Fluid Mech. 210 (1990) 537–563.
[14] Mutabazi I., Normand C., Wesfreid J.E., Gap size effects on centrifugally and rotationally driven instabilities, Phys. Fluids A-Fluid. 4 (1992) 1199–1205.
[15] Chandrasekhar S., Hydrodynamic and Hydromagnetic Stability, Oxford University Press, London, 1961.
[16] Carmi S., Tustaniwskyj J.I., Stability of modulated finite-gap cylindrical Couette flow: linear theory, J. Fluid Mech. 108 (1981) 19–42.
[17] Or A.C., Finite-wavelength instability in a horizontal liquid layer on an oscillating plane, J. Fluid Mech. 335 (1997) 213–232.
[18] Clever R., Schubert G., Busse F.H., Two-dimensional oscillatory convection in a gravitationally modulated fluid layer, J. Fluid Mech. 253 (1993) 663–680.
[19] Barenghi C.F., Jones C.A., Modulated Taylor–Couette flow, J. Fluid Mech. 208 (1989) 127–160.
[20] Ern P., Wesfreid J.E., Flow between time periodically co-rotating cylinders, J. Fluid Mech. (1999) (accepted for publication).